*Journal of Sound and Vibration* (1999) **219**(2), 193–205
*Article No*. jsvi.1998.1882, available online at http://www.idealibrary.com.on IDEAL

# OPTIMUM DESIGN OF A PASSIVE SUSPENSION SYSTEM OF A VEHICLE SUBJECTED TO ACTUAL RANDOM ROAD EXCITATIONS

J. A. TAMBOLI

*KIT's College of Engineering*, *Gokul Shirgaon*, *Kolhapur*-416 234, *India*

AND

S. G. JOSHI

*Walchand College of Engineering*, *Vishrambag*, *Sangli*-416 415, *India*

(*Received* 21 *March* 1997, *and in final form* 7 *July* 1998)

Vehicles are subjected to random excitation due to road unevenness and variable velocity. In most research work reported earlier, the response analysis for Mean Square Acceleration Response (MSAR) has been carried out by considering the power spectral density (PSD) of the road excitation as white noise, and the velocity of the vehicle as constant. However, in the present paper the PSD of the actual road excitation has been found to follow an approximately exponentially decreasing curve. Also the change in vehicle velocity has a significant effect on the values of Root Mean Square Acceleration Response (RMSAR). Therefore, in this work, the RMSAR of a vehicle dynamic system subjected to actual random road excitations is obtained so as to account for the effect of the actual PSD of road excitation and the frequent changes in vehicle velocity. The RMSAR of the vehicle is calculated for actual field excitation using the Fast Fourier Transformation (FFT) technique to obtain the PSD, by recording observations at the rear wheel. The effect of time lag due to wheelbase on the RMSAR of the vehicle is studied. For this purpose, a new ratio $\bar{\alpha}(\tau)$ has been introduced. The relationship between $\bar{\alpha}(\tau)$ and the autocorrelation has been formulated. This ratio is useful for considering the effect of time lag due to wheelbase on RMSAR. Similarly, the effect of vehicle velocity on the RMSAR is obtained.

Further, from a ride comfort point of view, the values of the design variables like spring stiffness and viscous damping coefficient of the front and rear suspensions have been obtained, by minimising the RMSAR using the desired boundary values of the vertical RMSAR as specified in the chart of ISO 2631, 1985(E) [1].



## 1. INTRODUCTION

The ride comfort characteristics of a vehicle dynamic system are influenced by the excitations due to road unevenness and variable velocity. These excitations are of the non-stationary random type. In earlier work on the analysis of vehicle response, the vehicle velocity was considered as constant, since it was difficult to

0022–460X/99/020193 + 13 $30.00/0 

introduce the effect of variable velocity in the formulation of the model for evolutionary PSD of the excitation due to road surface unevenness. Hammond and Harrison considered a single-degree-of-freedom quarter model for the vehicle dynamic system and have studied the response using a state space approach [2].

Karnopp considered the vehicle model as a single-degree-of-freedom quarter model with active and passive damping and linear stiffness, subjected to white noise base velocity excitation [3]. Sobczyk, Macvean and Robson have investigated stationary response to profile imposed excitation with randomly varying traverse velocity and showed that the change in velocity makes a proportional contribution to the response [4]. Duncan used a finite element analysis to improve the ride quality of a light duty truck, using an optimisation technique [5]. Hac and Youn showed that incorporation of a time delay between the front and rear axles in controller design improves the dynamic behaviour when road excitation is simulated by white noise and vehicle velocity is constant [6]. Elbehiery and Karnopp have optimised suspension system parameters, for five types of suspension systems, to obtain constant root mean square suspension deflection [7].

The characteristics of a vehicle dynamic system are influenced by (1) the excitations received by the vehicle due to road surface unevenness, (2) changes in the velocity of the vehicle, (3) time lag due to the wheelbase, and (4) the system parameters such as the spring constant and damping coefficient.

## 2. OBJECTIVES OF THE ANALYSIS

1. To analyse a given vehicle dynamic system subjected to actual road displacement type excitations recorded at the rear axle. Such an excitation will automatically take into consideration the effect of the change in PSD due to random road surface unevenness and variations in vehicle velocity. Also, the effect of time delay $\tau$ due to the wheelbase is considered at a given average vehicle velocity.

2. To study the effect of the vehicle velocity on the RMSAR of the vehicle.

3. To formulate an equation for the excitation PSD by fitting an exponential-type decreasing curve to the measured PSD obtained from the actual data using FFT analysis.

4. To minimise the RMSAR from a ride comfort point of view, using the desired boundary values of vertical RMSAR as specified in the chart of ISO 2631, 1985(E). The optimisation is carried out to obtain the design variables, namely the spring stiffness and viscous damping coefficient of the suspension system.

5. To compare the RMSAR of a vehicle subjected to actual road excitation with that predicted using the formulated equation for the PSD, for both the initial and optimal systems.

The analysis is restricted to a highway type of road condition.

## 3. VEHICLE MODEL

For the purpose of the above analysis, a two degree of freedom model is considered for half the vehicle and random road excitations of the displacement

type are recorded at the rear axle level. The half-car model considered in this paper is shown in Figure 1. The body structure of the vehicle is represented by the mass $M$ and the moment of inertia $I$ with respect to the central axis perpendicular to the vehicle's plane of symmetry. The vehicle is subjected to displacement excitations $q_1(t)$ and $q_2(t)$ respectively at the front and rear. Since there is a difference between amplitudes the $q_1(t)$ and $q_2(t)$, angular displacement about the mass center arises.

## 4. METHOD OF ANALYSIS

### 4.1. FORMULATION OF THE RATIOS $\alpha_a(\tau)$ AND $\bar{\alpha}(\tau)$

#### 4.1.1. *Formulation of the Ratio* $\alpha_a(\tau)$

The excitations at the front and rear axles of the vehicle at instant $i$ can be related by taking into account the effect of the time lag $\tau$ between $q_{1i}(t)$ and $q_{2i}(t)$, as

$$q_{1i}(t) = q_{2i}(t + \tau), \tag{1}$$

where $q_{1i}(t)$ and $q_{2i}(t)$ are displacement excitations respectively, at front and rear; $\tau$ = time delay = wheel base/velocity = $(L_1 + L_2)/v$; $L_1$ = the distance of mass centre from front axle; $L_2$ = the distance of mass centre from rear axle; $v$ = velocity of vehicle. A full list of nomenclature appears in the Appendix.

The value of the time delay $\tau$ varies with the vehicle velocity. The values $q_{2i}(t)$ and $q_{2i}(t)$ can be related by introducing a new ratio $\alpha_i(\tau)$ at the instant $i$ as

$$q_{2i}(t + \tau) = \alpha_i(\tau) q_{2i}(t). \tag{2}$$

From equations (1) and (2)

$$q_{1i}(t) = \alpha_i(\tau) q_{2i}(t), \qquad \alpha_i(\tau) = q_{1i}(t)/q_{2i}(t), \tag{3}$$

i.e.,

$$\alpha_1(\tau) = q_{21}(t + \tau)/q_{21}(t), \qquad \alpha_2(\tau) = q_{22}(t + \tau)/q_{22}(t), \ldots .$$

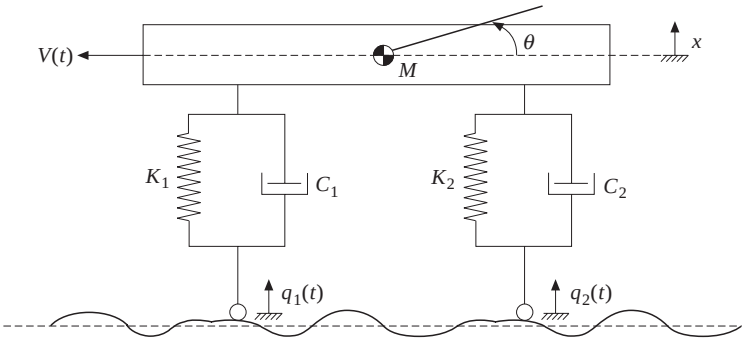


Figure 1. Two-DOF half car vehicle model.

The average value $\alpha_a(\tau)$ over the actual recorded sample is calculated as

$$\alpha_a(\tau) = \frac{1}{N}\sum_{i=1}^{N} \alpha_i(\tau) \quad \text{where} \qquad N \to \infty$$

$$\alpha_a(\tau) = \frac{1}{N}\sum_{i=1}^{N} \frac{q_{2i}(t+\tau)}{q_{2i}(\tau)}. \tag{4}$$

4.1.2. *Approximate Estimation of* $\bar{\alpha}(\tau)$

When a record of displacement excitation $q_2(t)$ versus time is available for a long duration of vehicle excitation, one can assume without loss of generality that instantaneous values of $\alpha_i(\tau)$ are replaced by their average value $\bar{\alpha}(\tau)$ of $\alpha_i(\tau)$ in the neighbourhood of the time instant $i$.

Then $\bar{\alpha}(\tau)$ can be written as:

$$\bar{\alpha}(\tau) \approx q_{21}(t+\tau)/q_{21}(t) \approx q_{22}(t+\tau)/q_{22}(t) \approx q_{23}(t+\tau)/q_{23}(t) \approx \cdots,$$

or alternatively as:

$$\bar{\alpha}(\tau) \approx q_{21}(t)q_{21}(t+\tau)/q_{21}^2(t) \approx q_{22}(t)q_{22}(t+\tau)/q_{22}^2(t) \approx \cdots. \tag{5}$$

Equation (5) can be written as

$$\bar{\alpha}(\tau) \approx \frac{q_{21}(t)q_{21}(t+\tau) + q_{22}(t)q_{22}(t+\tau) + \cdots}{q_{21}^2(t) + q_{22}^2(t) + \cdots} \tag{6}$$

Dividing the numerator and denominator by $N$, equation (6) can be written as

$$\bar{\alpha}(\tau) = \frac{1}{N}\sum_{i=1}^{N} q_{2i}(t)q_{2i}(t+\tau) \Big/ \frac{1}{N}\sum_{i=1}^{N} q_{2i}^2(t). \tag{7}$$

The autocorrelation function, $R(\tau)$, of the displacement excitation is

$$R(\tau) = \frac{1}{N}\sum_{i=1}^{N} q_{2i}(t)q_{2i}(t+\tau). \tag{8}$$

Using equation (8), equation (7) can be written as

$$\bar{\alpha}(\tau) = R(\tau) \Big/ \frac{1}{N}\sum_{i=1}^{N} q_{2i}^2(t) = \frac{R(\tau)}{E(q^2)} = \frac{R(\tau)}{R(0)} = \frac{R(\tau)}{\sigma^2}, \tag{9}$$

where $\sigma$ is the standard deviation, a measure of the spread about the mean value.

The value $\bar{\alpha}(\tau)$ obtained from equation 9 can be used to replace the $\alpha_a(\tau)$ of equation (4) for the approximate analysis of the non-stationary response of the vehicle.

To test the validity, an example of sinusoidal excitation will now be considered: using the function $A \sin(\omega t)$, the ratio $\bar{\alpha}(\tau)$ is given from equation (9) as $\bar{\alpha}(\tau) = \cos(\omega\tau)$. Figures. 2(a–c) show the comparison of $\alpha_a(\tau)$ and $\bar{\alpha}(\tau)$ using equations (4) and (9), for the case of sinusoidal excitation with $A = 1$, $f = 1$ Hz

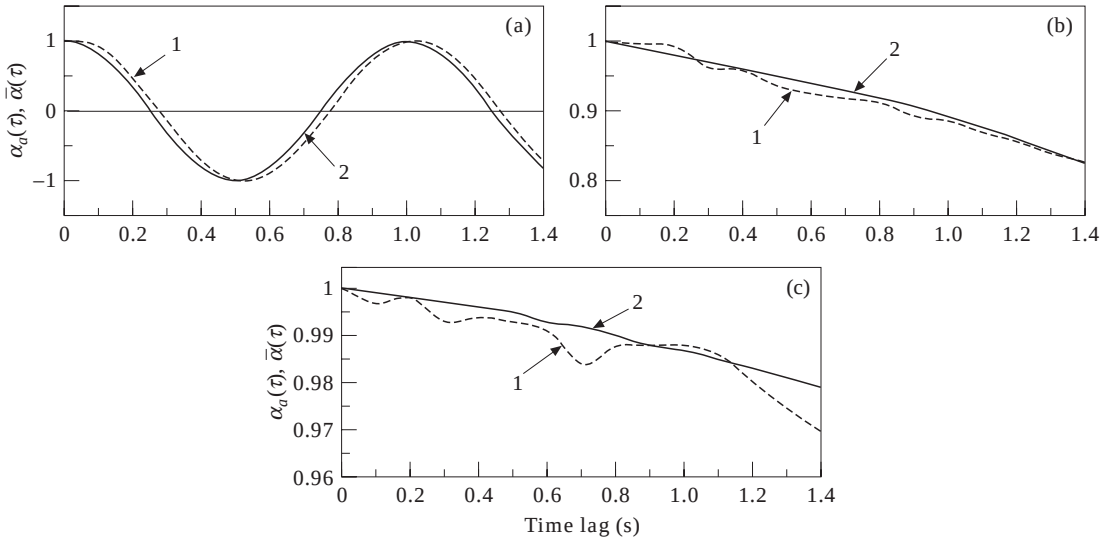


Figure 2. Comparison of $\alpha_a(\tau)$ and $\bar{\alpha}(\tau)$ for (a) sinusoidal excitation; (b) highway-type road excitation; (c) city-type road excitation. Key: 1, $\alpha_a(\tau)$; 2, $\bar{\alpha}(\tau)$.

at $t = 0{\cdot}1,\ 0{\cdot}2,\ 0{\cdot}3, \ldots$ and also for highway and city type road excitations respectively. These are drawn from the recorded data and given in Table 1.

The other methods which may be adopted to calculate the ratio $\bar{\alpha}(\tau)$ are

$$\bar{\alpha}(\tau) = \sqrt{\sum q_{1i}^2(t)} \Big/ \sqrt{\sum q_{2i}^2(t)}, \qquad \bar{\alpha}(\tau) = \sum q_{1i}(t) \Big/ \sum q_{2i}(t). \qquad \text{(10a, b)}$$

The values obtained by the above methods are also included in Table 1. Both from the figures and from Table 1, it can be seen that the actual value of $\alpha_a(\tau)$, obtained from equation (4), is in close agreement with the value $\bar{\alpha}(\tau)$ obtained from equation (9). Hence, the use of ratio $\bar{\alpha}(\tau)$ as given by equation (9) to obtain the RMSAR of the vehicle is discussed in the next part of the analysis.

## 5. VEHICLE TRANSFER FUNCTION ($\mathbf{H}(\mathrm{i}\omega)$)

The input–output relation for a linear system in the frequency domain is $\mathbf{H}(\mathrm{i}\omega)$, and the mean square response is given by:

$$E(\bar{x})^2 = \int_0^\infty |\mathbf{H}(\mathrm{i}\omega)|^2 G(\omega)\, \mathrm{d}\omega, \qquad (11)$$

where $G(\omega)$ is the PSD of excitation.

The equations of motion of a two-degree-of-freedom half car model, shown in Figure 1, are

$$\begin{aligned} M\ddot{x} + K_1(x - L_1\theta - q_1) + C_1(\dot{x} - L_1\dot{\theta} - \dot{q}_1) \\ + K_2(x + L_2\theta - q_2) + C_2(\dot{x} + L_2\dot{\theta} - \dot{q}_2) = 0, \\ I\ddot{\theta} - [K_1(x - L_1\theta - q_1) + C_1(\dot{x} - L_1\dot{\theta} - \dot{q}_1)]L_1 \\ + [K_2(x + L_2\theta - q_2) + C_2(\dot{x} + L_2\dot{\theta} - \dot{q}_2)]L_2 = 0. \end{aligned} \tag{12}$$

In order to study the effect of the time lag $\tau$ on the RMSAR of the vehicle, the ratio $\bar{\alpha}(\tau)$ is used to find the values of $q_1(t)$ in terms of $q_2(t)$ from $q_1(t) = \bar{\alpha}(\tau)q_2(t)$. Taking Laplace transforms, then substituting $i\omega$ for $s$ and putting the initial conditions as $x = 0$, $\dot{x} = 0$ at $t = 0$, equation (12) can be written in matrix form as:

$$\begin{bmatrix} K_1 + K_2 - M\omega^2 + i\omega(C_1 + C_2) & K_2L_2 - K_1L_1 + i\omega(-C_1L_1 + C_2L_2) & -K_1 - i\omega C_1 \\ K_2L_2 - K_1L_1 + i\omega(-C_1L_1 + C_2L_2) & K_1L_1^2 + K_2L_2^2 - I\omega^2 + i\omega(C_1L_1^2 + C_2L_2^2) & K_1L_1 + i\omega C_1L_1 \\ 0 & 0 & 1 \end{bmatrix} \begin{bmatrix} x/q_2 \\ \theta/q_2 \\ q_1/q_2 \end{bmatrix}$$

$$= \begin{bmatrix} K_2 + i\omega C_2 \\ K_2L_2 + i\omega C_2L_2 \\ \bar{\alpha}(\tau) \end{bmatrix}. \tag{13}$$

From this the required transfer function $\mathbf{H}(i\omega) = x/q_2$ can be calculated by inverting the complex matrix. Using this value of $\mathbf{H}(i\omega)$, the Mean Square Acceleration Response (MSAR) of the vehicle is:

$$E(\bar{\ddot{x}}^2) = (2\pi)^4 \int_0^\infty |\mathbf{H}(i\omega)|^2 G(f)\, df$$

## 6. FORMULATION OF AN EQUATION FOR POWER SPECTRAL DENSITY OF ROAD EXCITATION OBTAINED FROM RECORDED DATA

Figure 3 shows the measured displacement time history for highway and city type road excitations, captured at 10 samples per second. Figure 4 shows the PSD plot obtained from the recorded data using FFT analysis. It can be observed that this approximately follows an exponentially decreasing curve. Therefore the PSD of the road excitation cannot be considered as a white noise. As such, the PSD $G(f)$ of the road excitation can be approximated as:

$$G(f) = a^* \, e^{(-b^* f)} \tag{14}$$

## TABLE 1

*Comparison of $\alpha_a(\tau)$ and $\bar{\alpha}(\tau)$*

| $\tau(s)$ | $R(\tau)$ | $\alpha_a(\tau)$ (equation 4) | $\bar{\alpha}(\tau)$ (equation 7) | $\bar{\alpha}(\tau)$ (equation 10a) | $\bar{\alpha}(\tau)$ (equation 10b) | $\tau(s)$ | $R(\tau)$ | $\alpha_a(\tau)$ (equation 4) | $\bar{\alpha}(\tau)$ (equation 7) | $\bar{\alpha}(\tau)$ (equation 10a) | $\bar{\alpha}(\tau)$ (equation 10b) | $\tau(s)$ | $R(\tau)$ | $\alpha_a(\tau)$ (equation 4) | $\bar{\alpha}(\tau)$ (equation 7) | $\bar{\alpha}(\tau)$ (equation 10a) | $\bar{\alpha}(\tau)$ (equation 10b) |
|---|---|---|---|---|---|---|---|---|---|---|---|---|---|---|---|---|---|
| 0·00 | 0·500 | 1·00 | 1·00 | 1·00 | 1·00 | 0·00 | 70·938 | 1·00 | 1·00 | 1·00 | 1·00 | 0·00 | 220·763 | 1·00 | 1·00 | 1·00 | 1·00 |
| 0·10 | 0·404 | 0·899 | 0·809 | 1·00 | 6·462 | 0·10 | 70·274 | 0·997 | 0·991 | 1·00 | 1·00 | 0·10 | 220·463 | 0·997 | 0·999 | 1·00 | 1·00 |
| 0·20 | 0·154 | 0·454 | 0·309 | 1·00 | 1·732 | 0·20 | 69·753 | 0·994 | 0·983 | 1·00 | 1·00 | 0·20 | 220·332 | 0·998 | 0·998 | 1·00 | 1·00 |
| 0·30 | −0·155 | −0·164 | −0·309 | 1·00 | 1·843 | 0·30 | 69·197 | 0·969 | 0·975 | 0·999 | 0·999 | 0·30 | 220·135 | 0·993 | 0·997 | 1·00 | 1·00 |
| 0·40 | −0·404 | −0·719 | −0·809 | 1·00 | 2·742 | 0·40 | 68·594 | 0·965 | 0·967 | 0·999 | 0·999 | 0·40 | 219·895 | 0·994 | 0·996 | 1·00 | 1·00 |
| 0·50 | −0·500 | −1·00 | −1·00 | 1·00 | −16·036 | 0·50 | 67·999 | 0·947 | 0·959 | 0·999 | 0·999 | 0·50 | 219·621 | 0·993 | 0·995 | 1·00 | 1·00 |
| 0·60 | −0·404 | −0·898 | −0·809 | 1·00 | −0·542 | 0·60 | 67·428 | 0·938 | 0·951 | 0·999 | 0·998 | 0·60 | 219·316 | 0·991 | 0·993 | 1·00 | 1·00 |
| 0·70 | −0·154 | −0·453 | −0·309 | 1·00 | 0·168 | 0·70 | 66·848 | 0·932 | 0·942 | 0·999 | 0·998 | 0·70 | 218·974 | 0·984 | 0·992 | 1·00 | 1·00 |
| 0·80 | 0·155 | 0·164 | 0·309 | 1·00 | 0·412 | 0·80 | 66·206 | 0·928 | 0·933 | 0·999 | 0·998 | 0·80 | 218·606 | 0·988 | 0·990 | 1·00 | 1·00 |
| 0·90 | 0·404 | 0·719 | 0·809 | 1·00 | 0·498 | 0·90 | 65·459 | 0·911 | 0·923 | 0·998 | 0·997 | 0·90 | 218·213 | 0·988 | 0·988 | 1·001 | 1·001 |
| 1·00 | 0·500 | 1·00 | 1·00 | 1·00 | 0·345 | 1·00 | 64·604 | 0·906 | 0·911 | 0·998 | 0·997 | 1·00 | 217·791 | 0·988 | 0·987 | 1·001 | 1·001 |
| 1·10 | 0·404 | 0·899 | 0·809 | 1·00 | 6·467 | 1·10 | 63·667 | 0·892 | 0·898 | 0·998 | 0·997 | 1·10 | 217·354 | 0·986 | 0·985 | 1·001 | 1·001 |
| 1·20 | 0·154 | 0·454 | 0·309 | 1·00 | 1·732 | 1·20 | 62·680 | 0·881 | 0·884 | 0·998 | 0·997 | 1·20 | 216·915 | 0·980 | 0·983 | 1·001 | 1·001 |
| 1·30 | −0·155 | −0·164 | −0·309 | 1·00 | 1·843 | 1·30 | 61·671 | 0·867 | 0·869 | 0·998 | 0·997 | 1·30 | 216·468 | 0·974 | 0·981 | 1·001 | 1·001 |
| 1·40 | −0·404 | −0·719 | −0·809 | 1·00 | 2·742 | 1·40 | 60·669 | 0·857 | 0·855 | 0·998 | 0·997 | 1·40 | 216·017 | 0·969 | 0·979 | 1·001 | 1·001 |
| Sinusoidal type road excitation | | | | | | Highway type road excitation | | | | | | City type road excitation | | | | | |

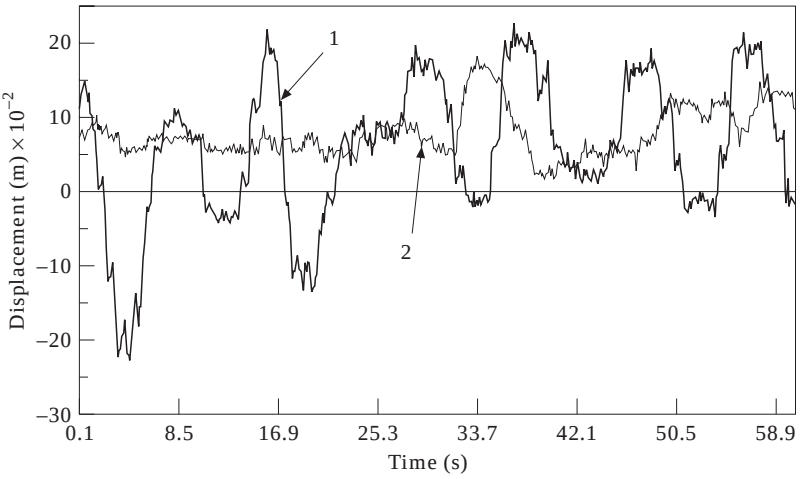


Figure 3. Displacement–time history. 1, highway-type road; 2, city-type road.

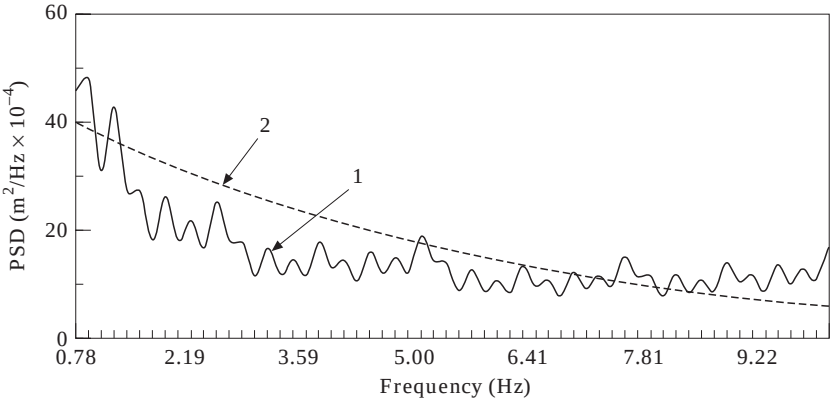


Figure 4. Comparison of PSD of actual (1) and formulated (2) road excitations.

where $f$ is the frequency in Hz. The values of variables $a$ and $b$ can be determined by minimizing the mean square error $E$, as follows:

$$\text{Minimised } E = \frac{1}{N} \sum (G_a^2(f) - a^* \, \mathrm{e}^{(-b^* f)}), \tag{15}$$

where $G_a(f)$ is the actual PSD of road excitation obtained from the recorded data and $N$ is total number of data points.

TABLE 2

*The values of variables a and b for equation* 14

| Road type | a ($m^2$/Hz) | b |
|---|---|---|
| Highway | $46{\cdot}85 \times 10^{-4}$ | 0·19 |
| City | $23{\cdot}0244 \times 10^{-4}$ | 0·213 |

TABLE 3

*The values of Gi and Wi from* ISO 2631, 1985(E) *for* 1 *min. duration* [1]

| Freq. (Hz) | 1 | 1·25 | 1·6 | 2 | 2·5 | 3·15 | 4 | 5 | 6·3 | 8 | 10 |
|---|---|---|---|---|---|---|---|---|---|---|---|
| RMSAR (m/s$^2$) | 5·6 | 5 | 4·5 | 4 | 3·55 | 3·15 | 2·8 | 2·8 | 2·8 | 2·8 | 3·55 |
| Weighting factor | 0·5 | 0·56 | 0·63 | 0·71 | 0·8 | 0·9 | 1·0 | 1·0 | 1·0 | 1·0 | 0·8 |

Using a standard curve fitting procedure and linear regression, the values of $a$ and $b$ are determined and given in Table 2. The PSD as formulated by using equation (14) is also shown in Figure 4.

The MSAR at each individual frequency is calculated in its 1/3 octave band as:

$$= (2\pi)^4 \int_{0{\cdot}89f}^{1{\cdot}12f} |\mathbf{H}(\mathrm{i}f)|^2 f^4 G(f)\, \mathrm{d}f. \tag{16}$$

The samples are recorded at a time interval of 0·1 s. Therefore, the sampling rate or sampling frequency $f_s$ is given as $= 1/\text{time interval} = 1/0{\cdot}1 = 10$ Hz while the Nyquist frequency is given as $f_h = f_s/2 = 5$ Hz. As aliasing does not exist for a discrete time signal [8], the frequency range for analysis is selected from 1–10 Hz. The RMSAR is calculated as the square root of the MSAR.

## 7. OPTIMUM DESIGN OF THE SUSPENSION SYSTEM

The optimum design of the suspension system from a ride comfort viewpoint can be obtained by selecting an objective function, $Z$, and taking the design variables as the spring constant and viscous damping coefficient of the front and rear suspensions. Taking the objective function $Z$ as given by Duncan [5]

$$Z = \text{minimise} \sum (W_i(\ddot{X}_i - g_i))^2 \tag{17}$$

TABLE 4

*The initial and optimal parameters of a heavy duty truck when* $wb = 5{\cdot}195$ m, $\tau = 0{\cdot}3$ s, *velocity* $= 62{\cdot}7$ km/h, $\bar{\alpha}(\tau) = 0{\cdot}975$

| | | Optimal values | |
|---|---|---|---|
| Parameter | Initial value | actual road excitation | formulated road excitation |
| $K_1$ (kN/m) | 465 | 255·75 | 274·35 |
| $C_1$ (kNs/m) | 16 | 10·4 | 11·04 |
| $K_2$ (kN/m) | 524 | 393 | 414 |
| $C_2$ (kNs/m) | 18 | 15·3 | 16 |

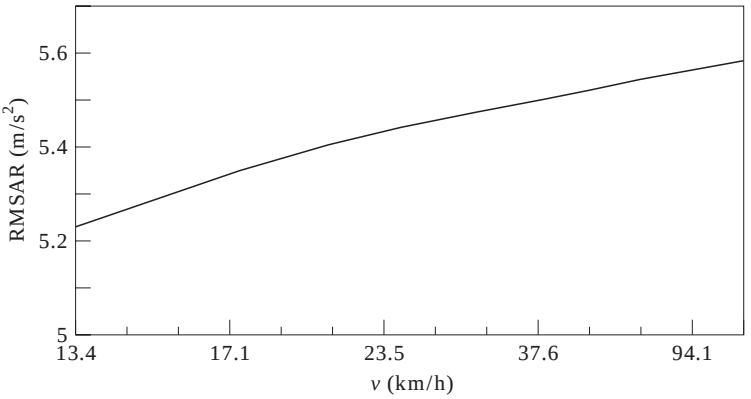


Figure 5. Effect of velocity on vehicle RMSAR.

where $W_i$ = weighting factor at $i$th frequency; $\ddot{X}_i$ = the vertical RMS acceleration at $i$th frequency from equation (16); $g_i$ = the desired value of RMS vertical acceleration at the $i$th frequency. The values of $W_i$ and $g_i$ are taken from the ISO 2631, 1985(E) chart and are given in Table 3.

The parameters of a Heavy Duty Truck vehicle model are taken as $M = 13\,200$ kg, $K_1 = 465$ kN/m, $C_1 = 16$ kNs/m; $K_2 = 524$ kN/m, $C_2 = 18$ kNs/m, $L_1 = 2{\cdot}340$ m, $L_2 = 2{\cdot}885$ m, wheel base $= 5{\cdot}195$ m, $K = 2{\cdot}310$ m.

The optimum values of design parameters of the suspension system are obtained for: i) actual road excitation; ii) PSD approximated as an exponentially decreasing curve.

A non-linear programming technique is used and optimum values so obtained are given in Table 4. Figure 7 shows the plot of RMSAR versus frequency for the optimal system.

## 8. RESULTS OF ANALYSIS

The relationship between $\bar{\alpha}(\tau)$ and the autocorrelation $R(\tau)$ of actual road excitation has been obtained and the $\bar{\alpha}(\tau)$ estimates are shown in Figs 2(a)–2(c). From these figures, it can be seen that the approximation is satisfactory.

Figure 4 shows that the PSD of the actual excitation decreases with frequency. It may be approximated as an exponentially decreasing form.

Figure 5 shows the effect of vehicle velocity on RMSAR for the parameters $wb = 5{\cdot}195$ m, $f = 5$ Hz, $\alpha_a(\tau) = 0{\cdot}969$, $\bar{\alpha}(\tau) = 0{\cdot}975$. It should be noted that for a human being the most sensitive frequency range is 4–8 Hz for longitudinal vibration. Therefore, the frequency selected for the analysis is 5 Hz [1]. From Figure 5, it can be seen that the RMSAR of the vehicle increases with the velocity and for the same $\tau$, the predictions made using $\alpha_a(\tau)$ and $\bar{\alpha}(\tau)$ respectively are found close. Figure 6 shows the effect of wheelbase on RMSAR for a velocity $= 62{\cdot}7$ km/h, $f = 5$ Hz. From this figure, it can be seen that the RMSAR decreases as the wheelbase increases.

The optimisation technique has been suggested for minimising the RMSAR of the vehicle suspension system, taking the same objective function as was used by

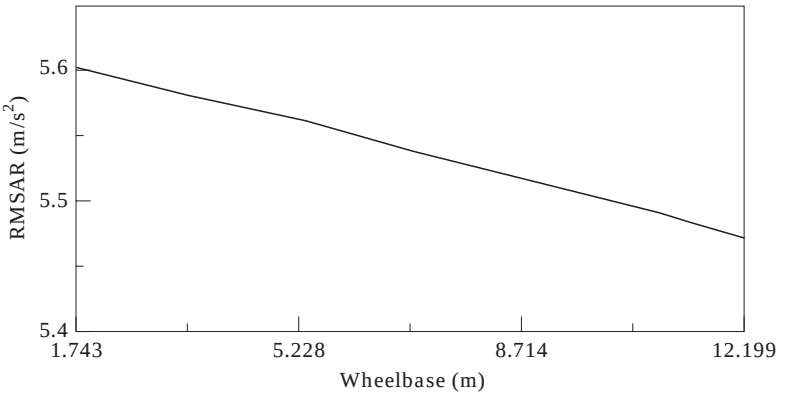


Figure 6. Effect of wheelbase on vehicle RMSAR.

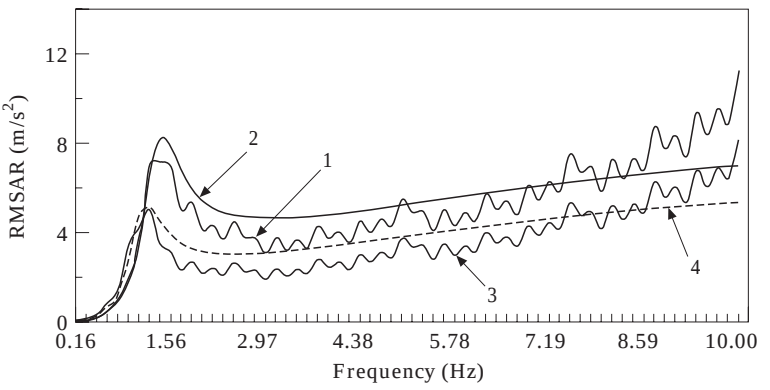


Figure 7. RMSAR of initial and optimal systems. Key: 1, Actual road excitation; 2, formulated road excitation: optimal system; 3, actual road excitation; 4, formulated road excitation.

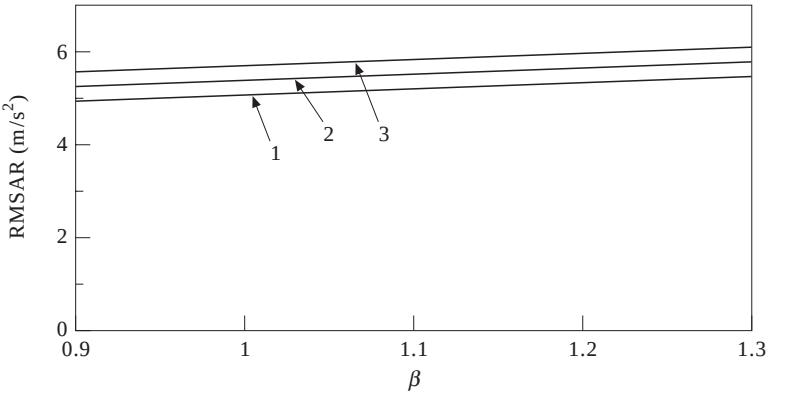


Figure 8. RMSAR versus $\beta$ ($\beta = K_2/K_1$, $\gamma = C_2/C_1$). Key: 1, $\gamma = 0{\cdot}9$; 2, $1{\cdot}255$; 3, $\gamma = 1{\cdot}35$.

Duncan [5]. This function uses the boundary values of the RMSAR, as defined in ISO 2631, 1985(E). The optimal values of the spring constant and damping coefficient of a heavy vehicle have been obtained, from a passenger ride comfort point of view, for a highway-type road condition. Figure 7 shows the plot of

RMSAR at different frequencies of excitation for $\tau = 0{\cdot}3$ s, $\bar{\alpha}(\tau) = 0{\cdot}975$, wheelbase = 5·195 m, for the initial and the optimal systems. Figure 7 shows that the RMSAR predicted using the formulated PSD function is in close agreement with that obtained using the actual measured and formulated excitation, for the initial as well as for the optimal system. Figure 8 shows the plot of RMSAR versus $\beta$, where $\beta = K_2/K_1$ for different values of $\gamma = C_2/C_1$. The values of the design variables such as spring stiffness and damping coefficient of sprung mass system can be obtained ($K_2$ and $C_2$), when $K_1$ and $C_1$ are known, for a desired RMSAR.

## 9. CONCLUSION

In this paper, a statistical, dimensionless ratio $\bar{\alpha}(\tau)$, a ratio of excitations at rear and from axle, has been formulated to study the effect of time lag $\tau$ on the response of the vehicle due to wheelbase. The relationship between $\bar{\alpha}(\tau)$ and the autocorrelation $R(\tau)$ of actual road excitation has been obtained and approximation is found to be satisfactory.

The ratio $\bar{\alpha}(\tau)$ is useful (i) when records of actual excitation are not available and only the type and form of excitation are known; (ii) when only a single record of excitation is available.

The ratio $\bar{\alpha}(\tau)$ varies between $-1$ and $+1$. For a vehicle with a given wheelbase, as the velocity increases, time lag $\tau$ decreases and the ratio $\bar{\alpha}(\tau)$ approaches unity. In this case, the excitations at the front and rear axles can be said to be approximately equal.

An optimisation technique has been suggested for minimising the RMSAR of the vehicle suspension system, by taking the desired boundary values of RMSAR as defined in ISO 2631, 1985(E).

The effect of vehicle velocity and wheelbase on the RMSAR has been studied and RMSAR is found proportional to the vehicle velocity and inversely proportional to its wheelbase. The results of the analysis presented in this paper can be used at the design stage of the vehicle suspension system, for approaching an optimised system right from the start. A similar type of analysis can be carried out by using recorded data for road excitation as the initial data and then employing the technique of optimisation for arriving at the suspension system parameters. The objective function may be taken as a combination of ride comfort and ride safety, by taking appropriate weighting factors.

## REFERENCES

1. International Standard Organisation 1990 *ISO* 2631, 1985(E). Mechanical vibration and shock; 481–495.
2. J. K. Hammond and R. F. Harrison 1981 *Journal of Dynamic System Measurement and Control* **103**, 245–250. Non-stationary response of vehicle on rough ground—a state space approach.
3. D. Karnopp 1989 *Journal of Acoustic, Stress and Reliability in Design* **111**, 278–283. Analytical results for optimum actively damped suspension under random excitation.
4. K. Sobczyk, D. B. Macvean and J. D. Robson 1977 *Journal of Sound and Vibration* **52**, 37–49. Response to profile imposed excitation with randomly varying traversal velocity.

5. A. E. DUNCAN 1982 *Society of Automotive Engineers* **811313**, 4075–4089. Application of modal modelling and mount system optimization to light duty truck ride analysis.
6. A. HAC and I. YOUN 1993 *Journal of Vibration and Acoustics* **115**, 498–508. Optimal design of active and semi-active suspensions including time delays and preview.
7. E. M. ELBEHEIRY and D. C. KARNOPP 1996 *Journal of Sound and Vibration* **189**, 547–564. Optimal control of vehicle random vibration with constrained suspension deflection.
8. G. E. CARLSON 1992 Signal and Linear system Allied Publishers Limited, MUMBAI 647–710.

## APPENDIX: NOMENCLATURE

| | |
|---|---|
| $M$ | mass in kg. |
| $K_1$ | stiffness of spring of front side in kN/m |
| $C_1$ | damping factor of front side in kNs/m |
| $K_2$ | stiffness of spring of Rear side in kN/m |
| $C_2$ | damping factor of Rear side in kNs/m |
| $K$ | radius of gyration in m |
| $q_1$ | excitation at rear side |
| $q_2$ | excitation at front side |
| $\mathbf{H}(\mathrm{i}\omega)$ | transfer function |
| $\omega$ | excitation frequency in rad/s |
| $f$ | excitation frequency in Hz |
| $L_1$ | the distance of mass centre from front axle |
| $L_2$ | the distance of mass centre from rear axle |
| $G(f)$ | Power Spectral Density (PSD) at frequency $f$ |
| $E[\cdot]$ | expectation |
| $\tau$ | time lag in s |
| $v$ | vehicle velocity in km/h |
| $\alpha_a(\tau)$ | actual ratio of excitation at front and rear wheel excitation at time lag $\tau$ |
| $\bar{\alpha}(\tau)$ | average ratio of excitation at front and rear wheel excitation at time lag $\tau$ |
| $wb$ | wheelbase in m |